Fuel Processing Technology 175 (2018) 26–34

Contents lists available at ScienceDirect

Fuel Processing Technology

journal homepage: www.elsevier.com/locate/fuproc

Preliminary understanding on the ash behavior of algae during co-gasification in an entrained flow reactor

Youjian Zhu[a], Philip J. van Eyk[b], Christoffer Boman[c], Markus Broström[c], Kawnish Kirtania[d], Patrycja Piotrowska[c], Dan Bostrom[c], Rocky de Nys[e], Sankar Bhattacharya[f], Francesco G. Gentili[g], Peter J. Ashman[b,*]

[a] School of Energy and Power Engineering, Zhengzhou University of Light Industry, Zhengzhou, Henan 450002, China
[b] School of Chemical Engineering, University of Adelaide, Adelaide, SA 5005, Australia
[c] Thermochemical Energy Conversion Laboratory, Department of Applied Physics and Electronics, Umeå University, 901 87 Umeå, Sweden
[d] Department of Chemical Engineering, Bangladesh University of Engineering and Technology, Dhaka 1000, Bangladesh
[e] MACRO, The Centre for Macroalgal Resources and Biotechnology, and College of Science and Engineering, James Cook University, Townsville, QLD 4811, Australia
[f] Department of Chemical Engineering, Monash University, VIC 3800, Australia
[g] Department of Wildlife, Fish, and Environmental Studies, Swedish University of Agricultural Sciences (SLU), 901 83 Umeå, Sweden

ARTICLE INFO

Keywords:
Algae
Ash behavior
Co-gasification
Fouling
Ash transformation

ABSTRACT

Algae are considered as a promising alternative fuel to produce energy due to its advantages such as high production yield, short growth cycle and flexible growing environment. Unfortunately, ash-related issues restrict its thermochemical utilization due to the high ash content and especially the high alkali metal concentration. In this paper, the gasification performance and ash behavior were experimentally analysed for three macro- and micro-algal species. Clear differences in the proximate and ultimate compositions were found between the cultivated algae used in this study and macroalgae (seaweed) harvested from the marine environments. Algal biomass generally contained higher Na and P contents than lignocellulosic biomass. Microalgae also had a relatively high mineral content due to the impurities in the harvesting process which included centrifugal pumping followed by sedimentation. Co-gasification of 20 wt% algae with softwood was investigated using an entrained flow reactor. The addition of both macroalgal species *Derbersia tenuissima* and *Oedogonium* to softwood had a limited influence on the gas yields and carbon conversion. On the other hand, the addition of the microalgal species *Scenedesmus* significantly decreased the main gas yields and carbon conversion. Moreover, the addition of algae clearly changed the residual ash composition of the base fuel. Finally, a preliminary understanding of the ash behavior of the tested algae blends was obtained through the analysis of the fuel ashes and the collected residual ashes. Fouling and corrosion were presumably occurred during the co-gasification of wood/macroalgae blends in view of the high alkali metal content. Microalga *Scenedesmus* had a high mineral content which could potentially capture the alkali metal in the ash and mitigate fouling when gasified with softwood. The growing environment and harvesting method were found to be significantly affecting the ash behavior implying the need for careful consideration regarding co-gasification process.

1. Introduction

Biomass is a carbon neutral renewable energy source which has the potential to replace fossil fuels in all areas of energy utilization, e.g. heat and electricity production, chemicals and liquid fuels synthesis [1]. Algae, including both microalgae and macroalgae, are considered as a promising alternative biomass to traditional terrestrial feedstocks to produce energy due to their high production yield, short growth cycle and flexible growing environment [2].

The harvested algae generally have a high moisture content as a result of cultivation conditions. Consequently, research of algae-to-energy has focused on anaerobic digestion [3,4], fermentation [5], hydrothermal liquefaction [6,7], and hydrothermal gasification [8] as these processes can successfully utilize feedstocks with a high moisture content. However, anaerobic digestion and fermentation usually need a long reaction time with a comparatively low conversion rate compared to thermochemical conversion methods [9]. Additionally, hydrothermal liquefaction/gasification technologies are currently immature,

* Corresponding author.
E-mail address: peter.ashman@adelaide.edu.au (P.J. Ashman).

https://doi.org/10.1016/j.fuproc.2018.02.028
Received 12 November 2017; Received in revised form 12 February 2018; Accepted 28 February 2018
Available online 07 March 2018
0378-3820/

and considerable technical difficulties need to be overcome prior to broad industrial-scale application. On the other hand, the development of drying technologies and the proposition of integrated drying, gasification, and combined cycle electricity generation substantially decreases the need for external energy in the drying of algae [9,10]. This makes conventional gasification (hereafter referred to as gasification) a promising method considering its maturity, and reliability, in addition to the advantages of a high conversion efficiency and low reaction time.

Current gasification technologies mainly include fixed bed, fluidized bed and entrained-flow gasification [11]. Among them, entrained-flow technology has advantages of larger throughput, faster reaction rate and higher conversion efficiency compared to fixed bed and fluidized bed processes. During the conversion process, the inorganic species in the fuels tend to form molten substances and release to the gas phase under high temperature [12,13]. These gas phase inorganics subsequently condense on the colder parts of the system and cause operating problems such as fouling. Several studies [14–18] have been conducted to investigate the ash transformation and behaviors of inorganics during the entrained-flow biomass combustion and gasification with the aim of the alleviation of ash-related operating difficulties. These works generally focus on the woody biomass [16,18] and agricultural residues such as straw [15,17] and corn stover [15,18]. Entrained-flow gasification of straw [14] indicated that approximately 40% of K and 70% of Na in the fuel ash transformed into the gas phase at the operating temperature of 1200 °C. Simon Leiser et al. [15] found that most of K, Cl, and S are released into the gas phase and formed sub-micrometer particles < 0.5 μm during entrained flow gasification of straw and corn stover. In the case of corn stover, large fraction of K was retained in the ash/slag due to the abundance of aluminosilicates and lower Cl content in the fuel ash [15].

Algal biomass generally has a high ash and also alkali metal (both K and Na) content due to the specific cultivation environment and harvesting method [19]. Therefore, the ash content and composition of algae differs significantly from that of woody biomass and agricultural residues [20]. Different inorganic transformations and ash formation behaviors have been observed during the thermochemical conversion process. The release of K, Na, P, Cl, S of one macroalga (*Oedogonium* sp.) and two microalgal species (a polyculture species TPC and *Tetraselmis* sp.) during the thermochemical process were studied in a fixed bed reactor [21]. Lane et al. [21] found that approximately 20% of the K, 30–40% of the Na and almost all Cl and S and were released at 1000 °C for *Oedogonium* and *TPC*. For *Tetraselmis*, the release of alkali metal was 60–100% at 1000 °C due to the existence of high amount of Cl in the fuel. The high release ratio of alkali metals, Cl and S in combination with the high ash content may cause operating difficulties during the gasification process, e.g. agglomeration, fouling and deposition. Pure algae gasification in fluidized bed reactor was unsuccessful due to the rapid bed sintering and ash agglomeration [22]. Therefore, co-gasification of algae with coal/biomass has been proposed [19,23] to mitigate the ash related problems during pure algae gasification. Zhu et al. [19] found that bed agglomeration was significantly improved during co-gasification of algae with Victorian brown coal. The gasification tests lasted for 4 h without defluidization for co-gasification of *Derbersia* and *Oedogonium* with brown coal. Meanwhile, research [24] indicated that synergetic effects exist during the co-utilization of algae with other fuels. The algal char had a catalytic effect on the degradation of the textile dyeing sludge and increased the burnout rate [24]. Moreover, as a relatively new biofuel, algae-related infrastructure is currently still underdeveloped. Co-utilization of small amount algae could also facilitate the development of algae-related infrastructure and lay a foundation for the algae only system. Therefore, research on the co-gasification of algae has received increasing attentions in the past decade [19,22,23,25–27].

Although works related to co-gasification of algae with other fuel has been published previously, they were generally conducted in fixed bed/thermogravimetric analyzer [26,27] and fluidized bed [19,22,23,25]. Given the differences of temperature, gas velocity and fuel particle size in the reaction zone, the ash formation in entrained-flow reactor differs markedly from those in fixed bed and fluidized bed [18]. Previous research [28,29] indicated that the release of K, Na and S for wood chips increased as the bed temperature increased. Frandsen et al. [16] concluded that the total inorganics released from pulverized fuel-fired furnace were markedly higher than that from the fixed bed. It was also observed [17,18] that fly ash from straw suspension firing contained mainly Si, K and Ca, while fly ash straw grate firing was mainly composed of volatile elements K, and Cl. Similar compositional difference of deposits was also seen for these two gasification technologies [18]. So obviously the experience from fixed bed, fluidized bed and pulverized fuel-fired furnaces cannot be directly extrapolated for the entrained flow reactor. However, to the best of the authors' knowledge, research on ash behavior in entrained flow gasification of algae is scarce and thus corresponding research is needed.

Entrained flow gasification tolerates 40 wt% ash at the maximum for the dry feed gasifer whereas the gasification efficiency decreases notably with the increase of ash content [30]. Therefore, co-gasification of small amount of algae (20 wt%) with softwood (ash content 0.3 wt%) in an entrained flow reactor was conducted in this study considering the high ash content of algae especially microalgal species. This research has several aims. These are: 1) identify the difference of the fuel properties between the algae and lignocellulosic biomass fuels; 2) investigate the effects of the addition of algae to lignocellulosic biomass on gas yields and carbon conversion; and 3) investigate the effects of the addition of algae on the ash behavior to understand ash transformation in the algae co-gasification process.

2. Experimental

2.1. Fuels

The fuels employed in this study include: softwood pellets and three species of algae. The wood pellets (hereafter referred to as WD), which is a commercial softwood pellet of pine and spruce, is mainly used for small-medium scale heating applications as well as a large-scale combined heat and power system in Sweden [23].

The two species of macroalgae, *Derbersia tenuissima* (hereafter referred to as Deb) and *Oedogonium intermedium.*, were cultivated in tanks at the Marine & Aquaculture Research Facilities (James Cook University, Townsville, Queensland, Australia). *Oedogonium* was cultured in both high (~12 $mg{\cdot}L^{-1}$) and low (< 0.1 $mg{\cdot}L^{-1}$) nitrogen conditions and the corresponding harvested algae are referred to as *Oedogonium* N+ (hereafter referred to as ODN+) and *Oedogonium* N- (hereafter referred to as ODN-). The species were chosen as they are targets for the treatment of waste-water. *Derbesia* is a marine species and has application in the bioremediation of waste-water from land-based marine aquaculture, for example shrimp and marine fish. *Oedogonium* is a freshwater species and has broad application in the treatment of waste-water from municipal water treatment and intensive agriculture [31]. More importantly, both *Derbesia* and *Oedogonium* have a high productivity [31,32] and have been identified as a feedstock for energy production [33,34]. The microalga *Scenedesmus* sp. (hereafter referred to as SA), which was cultivated in the algae pilot plant at Swedish University of Agricultural Sciences (Umeå, Sweden), has been tested for municipal and industrial wastewater treatment in the Umeå – ÖrnskÖldsvik region. Detailed information about the growing conditions and harvesting method of the employed algae is presented elsewhere [19,35,36]. The proximate analysis, ultimate analysis, heating value, and ash elemental analysis of the algal samples and softwood are shown in Tables 1 and 2, respectively. The as received samples were milled using a knife mill and sieved to 100–250 μm for the following experiments. The blends of wood/algae were prepared by homogenously mixing 20 wt% algae and 80 wt% of wood. Table 1 presents the proximate analysis, ultimate analysis, and heating value of

Table 1
Proximate, ultimate analysis and high heating values of the fuels used.

	WD	Deb	ODN +	ODN-	SA
Higher heating value, MJ/kg db[a]	20.7	20.5	19.1	18.3	15.4
Moisture content, %	7.0	7.0	7.0	7.0	7.0
Proximate analysis (wt% db[a])					
volatile matter	85.6	73.2	75.3	76.2	54.3
fixed carbon	14.1	14.9	17.4	16.2	7.9
ash	0.3	11.9	8.1	7.9	37.8
Ultimate analysis (wt% db[a])					
C	51.4	46.6	46.0	44.6	32.6
H	6.2	6.1	6.0	5.8	4.7
O, by difference	42.0	26.9	35.4	39.3	19.3
N	0.1	6.11	3.93	1.84	4.2
S	0.01	0.9	0.2	0.18	0.97
Cl	0.01	1.53	0.36	0.41	0.39

[a] db = dry basis, WD = wood pellets, Deb = Derbersia tenuissima, ODN + = *Oedogonium* N +, ODN- = *Oedogonium* N-, SA = *Scenedesmus* sp.

Table 2
Ash elemental analysis of the employed fuels.

mg/kg of dry fuel	WD	Deb	ODN +	ODN-	SA
Na	8	14,000	13,000	14,000	3100
Mg	139	4700	3800	2800	12,000
K	359	7300	13,000	13,000	8700
Al	26	100	155	85	19,000
Si	91	7100	1000	1300	63,000
P	40	5800	9600	4800	11,000
S	53	9030	1980	1810	9700
Cl	0.02	15,260	3590	4090	3900
Ca	686	22,000	4400	4800	41,000
Fe	24	1800	1800	1300	36,000
Mn	81	56	80	62	2300
Zn	8	70	87	67	2200
Ti	3	14	13	18	1600

the employed fuels.

2.2. Gasification experiments

The gasification tests were conducted in an entrained flow reactor using sub-stoichiometric air as gasifying agent. The schematic diagram of the experiment rig is shown in Fig. 1. It is composed of a gas supply system, a fuel feeding system, a quartz reactor, and a sampling and analysis system. The gas supply system includes gas cylinders, mass flow meters and associated piping with valves. The reactor is a 2 m length quartz tube with two concentric layers. The inner diameter and outer diameter are 50 and 80 mm, respectively. It is electrically heated by 6 external temperature programmed heating elements which provide an isothermal temperature inside the reactor. Fuel was fed into the reactor using a piezoelectric feeder once the reactor was heated to the desired temperature. A water-cooled injector was used to avoid overheating of the fuel. The carrier gas (a mixture of N_2 and air) was fed at 1 L/min together with the fuel directly into the internal reaction chamber. On the other hand, the primary gas (N_2) was fed at 4 L/min into the external reactor chamber, in which it would be heated and then entered into the internal reaction chamber. The particle residence time, which was calculated following Umeki et al. [37], varies between 5 and 6 s due to the density difference of the fuels. After the reaction, the solid residues (predominantly ash with tiny amount of unburned char) were collected in a glass container and the product gas passed through an ice bath and a thimble filter sequentially to remove tar and ultra-fine particles. The gas composition was measured by an on-line micro-GC. The operating conditions of the gasification tests are provided in Table 3. Repeated experiments were conducted and the standard deviations indicated that the reproducibility is in acceptable range.

2.3. Ash samples characterization

The collected residual ashes were characterized by scanning electron microscopy (SEM) with energy dispersive X-ray (EDX) along with X-ray Diffraction (XRD) techniques. SEM/EDX (Philip XL30) analyses were conducted in BSE mode to provide an understanding of the morphology and the elemental composition of the residual ash. Three different areas (100 × 100 μm) were analysed for each residual ash sample and an averaged value was calculated to estimate the composition. Several spot analyses were performed to obtain the composition of the representative ash particles. The crystalline phases contained within the residual ash samples were analysed with a D8 Advance Bruker XRD instrument in θ-θ mode, with an optical configuration consisting of a line-focus tube, Cu Kα radiation and a Vantec-1 detector. The detailed operational and pattern figure analysis method were reported in our previous work [19,23].

3. Results and discussion

3.1. Fuel properties

In order to compare the fuel properties of the used algae with other solid fuels (especially algal biomasses from the previous research [38,39]), the proximate and ultimate analysis of the fuels used in this study and various solid fuels from literature [38–40] are plotted in the ternary diagram shown in Figs. 2 and 3, respectively. It should be noted that the macroalgae in the literature, which were directly harvested from the marine environment, have a different cultivation environment from the employed algae in this research. The employed macroalgae species, including Derbersia and the two Oedogonium (N + and N-), generally have lower fixed carbon content and higher volatile content compared to algal biomass harvested from marine environment. They are located at the top-left corner in the chart and are close to the lignocellulosic biomass with slightly higher ash content. Unlike macroalgae, the microalga *Scenedesmus* has an extremely high ash content of 37.8% due to the impurities (sand and in some case fine gravel particles) in the harvesting process which included centrifugal pumping followed by sedimentation. With regard to the elemental composition, the lignocellulose biomass generally has a concentrated distribution while algae biomass distributes dispersedly in the chart. The macroalgae harvested from the marine environment mostly have a higher O and (N + S + Cl) content than the used algae. Although the used algae (including both marco- and micro-) are situated close to the lignocellulose, they generally have a higher (N + S + Cl) content.

Ash compositions of various solid fuels are presented in Fig. 4. It can be observed that the coal generally contain higher (Al_2O_3 + Fe_2O_3 + MnO + TiO_2) content in their ash than the biomass (including the lignocellulosic biomass and algal biomass). This can be attributed to the large amounts of the inorganic minerals such as clay and pyrite [41,42] in typical coals. Biomass generally has a high (Na_2O + K_2O + CaO + MgO) as these elements (except of Na) are essential for the growth of the plants that the biomass fuels originate from. The used macroalgae are located at the top-right corner in the chart and the (Na_2O + K_2O + CaO + MgO) content accounts for approximately over 70% of the ash. It can be observed in Table 2 that Na content is relatively high in the used algae. This high Na content in algae results mainly from the high Na content in the cultivation environment or the nutrients used during its growing process [19]. Although the algae and the lignocellulosic biomass are plotted in the same group in Fig. 4, it should be noted that algae generally have a higher Na and P content than lignocellulosic biomass (as shown in Table 2). Previous research [20] indicated that Na and P in the algal species are mostly in water-leachable form which are relatively reactive during the thermochemical reaction. Similar to K, Na in the fuel is highly reactive and Na-species are predominantly released to gas phase and cause operating difficulties such as fouling and corrosion. Additionally, the

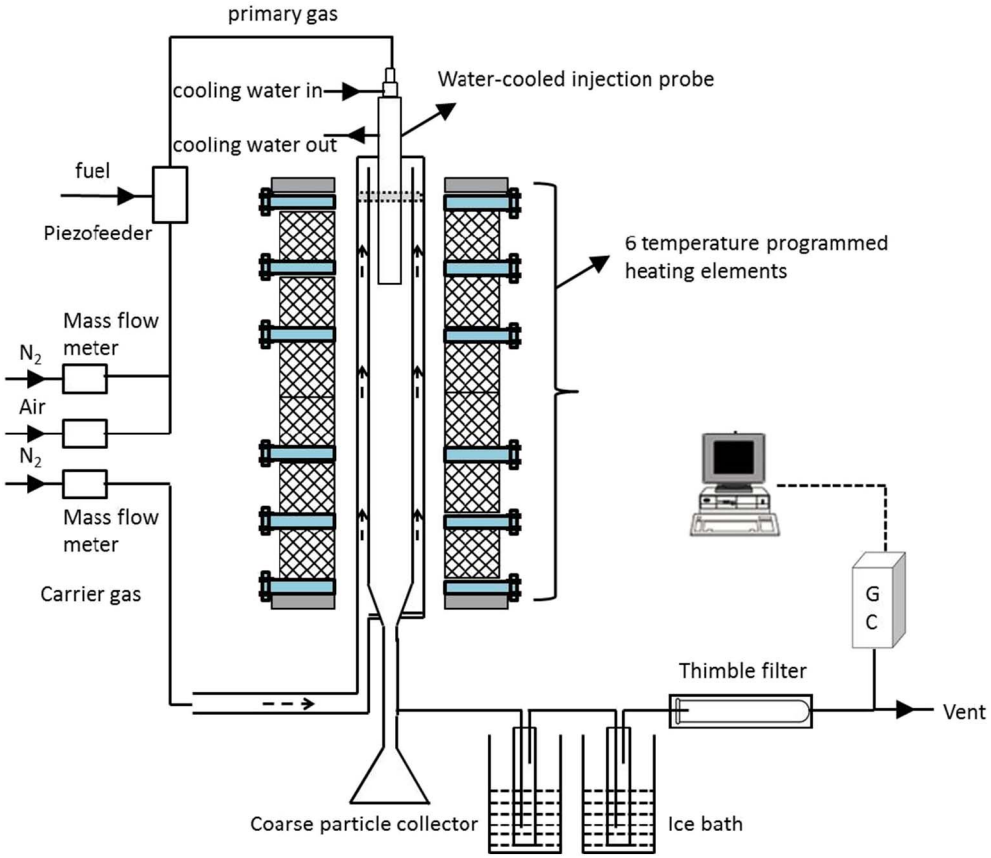

Fig. 1. Schematic diagram of the experimental rigs.

formation of low-melting temperature eutectic mixture will also be enhanced. The existence of P could reduce the evaporation of K/Na to gas phase by fixing it in different forms of phosphates [43–45]. However, the influence on ash melting behaviour is rather complex and is closely dependent on the alkali earth metal content and P/K ratio in the fuel [43,44,46,47]. The detailed influence of Na and P in the macroalgae will be discussed in the following part. Microalga *Scenedesmus* situates closely to coal in the chart as it has a high content of Al_2O_3, Fe_2O_3 and SiO_2. This is linked to its particular culture conditions (municipal and industrial wastewater) and the impurities (sand and fine gravel particles) infiltrating during the harvesting process [19,23].

3.2. Effect of algae addition on gasification performance

The main gas yields and carbon conversion of wood and WD/algae co-gasification tests are presented in Fig. 5 and Table 3, respectively. It can be observed that the carbon conversion rates were higher than 85% except of WD/SA. Considering that the rates were calculated without considering light hydrocarbons, the actual values would be even higher. Additionally, the EDX analysis indicated that the carbon contents of the residues are < 10% (data not presented) which implies complete reaction. The low carbon conversion rate of WD/SA were also found in the previous fluidized bed gasification studies [19,23]. The possible reasons are: 1) the deactivation of alkali metals through the formation of silicates with a high Si content in the ash for the microalgae addition; and 2) the reduction of active sites due to high ash content of SA [19]. The addition of 20 wt% *Derbersia* in softwood has no significant effects on the gas yields and carbon conversion. For the two WD/OD blends, the CO yield increases slightly (< 5%) with a substantial decrease of H_2 yields (25–29%), and the carbon conversions are also slightly increased by < 5%. The addition of 20 wt% microalga *Scenedesmus* remarkably decreases the CO and H_2 yields by 18 and 37%, respectively, with a decrease of carbon conversion by 17% in comparison with wood. It should be mentioned that the H_2 yield decreases to various extents with the addition of algae. This can be attributed to the fact that the higher lignin content in woody biomass, compared to herbaceous and aquatic

Table 3
Operating parameters and typical gasification results of the gasification experiments.

	WD	WD/Deb	WD/ODN+	WD/ODN-	WD/SA
Furnace temperature, °C	1000	1000	1000	1000	1000
Primary gas flow rate, air, ml/min	165	327	173	280	287
Primary gas flow rate, N_2, L/min	0.9	0.7	0.9	0.9	0.8
Carrier gas flow rate, L/min	4.0	4.1	4.1	4.1	4.0
Fuel feeding rate, g/h	7.5	14.7	9.6	14.3	13.2
O/C, molar ratio	0.6	0.7	0.6	0.6	0.7
H_2O/C, molar ratio	0.1	0.1	0.1	0.1	0.1
Syngas yield, Nm^3/kg	1.3 ± 0.19	1.3 ± 0.21	1.1 ± 0.10	1.1 ± 0.15	0.9 ± 0.13
Heating value of syngas,	9.7 ± 0.26	10.2 ± 0.45	10.3 ± 0.19	10.2 ± 0.3	9.6 ± 0.37
Carbon conversion, %	85.4 ± 13.4	86.8 ± 14.6	89.2 ± 6.2	88.0 ± 9.4	71.2 ± 7.1

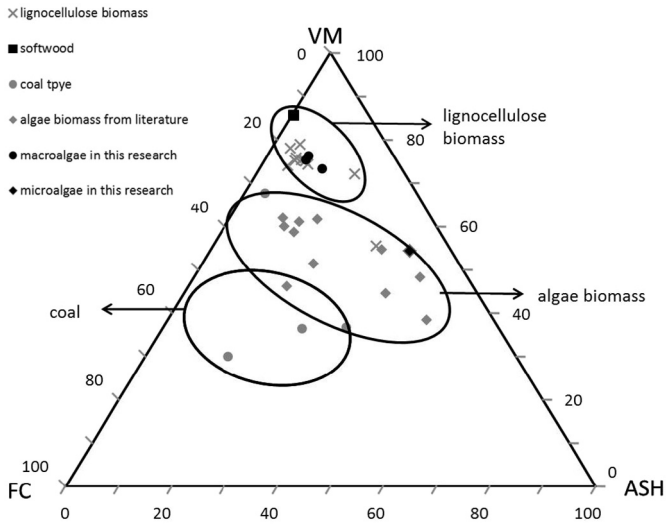

Fig. 2. Ternary diagram of proximate composition of various solid fuels, wt%.

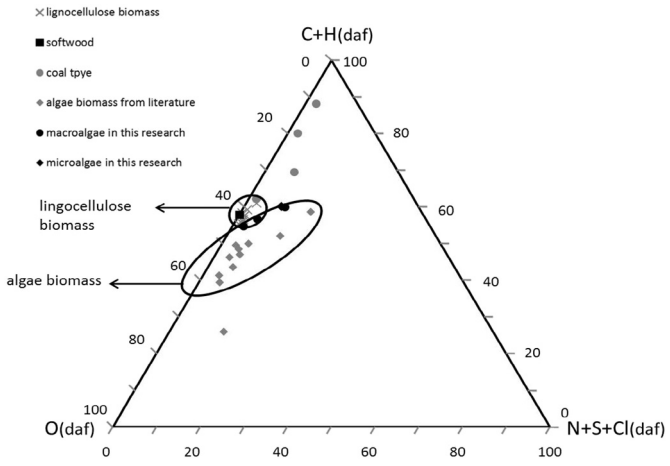

Fig. 3. Ternary diagram of ultimate composition of various solid fuels, wt%.

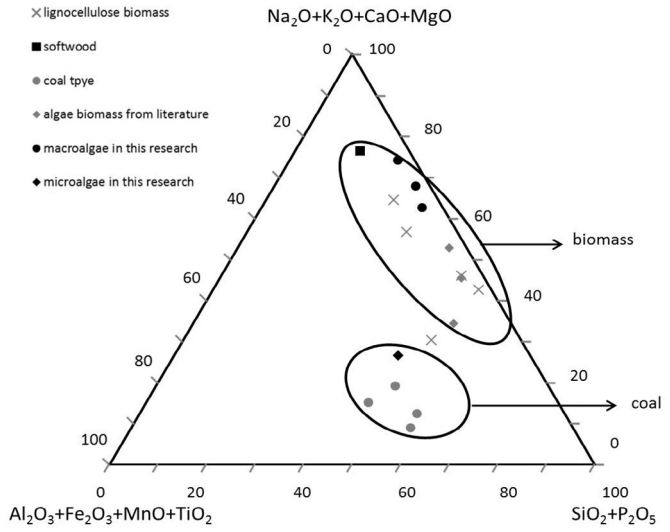

Fig. 4. Ternary diagram of ash elemental composition of various solid fuels, wt%.

biomass, favors the formation of H_2 during the gasification process [48,49]. In summary, the addition of macroalgae in wood has a less significant influence on the carbon conversion rate and gas yields which implies the potential utilization of marcroalgae in the co-gasification process with softwood.

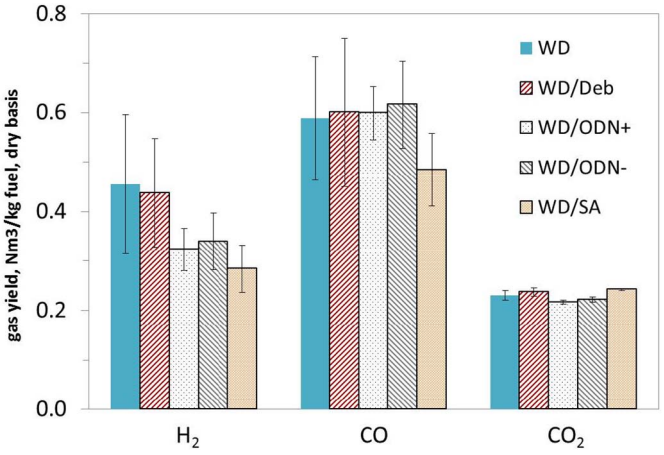

Fig. 5. Main gas yields of softwood and WD/algae tests.

3.3. Ash characterization

The compositions and crystalline phases present in the residual ash from softwood and WD/algae co-gasification tests are presented in Fig. 6 and Table 5, respectively. It can be noted that S and Cl content from wood ash was surprisingly high considering its values in the fuel. This could be due to deposition of KCl and K_2SO_4 on the ash particles during the cooling process which causes the overestimation of Cl and S content from EDX [50]. The residual ash of the wood test is mainly composed of Ca, Si, S, and K in decreasing order. XRD analysis indicates that the crystalline phases present in the ash are mainly composed by $CaCO_3$ and $Ca_5(PO_4)_3OH$ with a minor contents of KCl. The addition of macroalgae clearly increases the alkali metals (especially Na) and P content with a decrease of Ca and S content. The crystalline phases also changed significantly. For WD/Deb, Ca-containing compounds as Ca $(OH)_2$, $CaCO_3$, ZSM-12/11,$CaKPO_4$ were abundant in the crystalline phase with a minor content of MgO, NaCl and a trace amount of $K_3Na(SO_4)_2$, SiO_2. The crystalline phases in the two WD/*Oedogonium* ashes are quite similar with $CaKPO_4$, MgO, SiO_2 as the main phases. Additionally, certain amount of K/Na containing crystalline phases was detected in the wood/macroalgae tests (e.g. Na_3PO_4, $K_3Na(SO_4)_2$, and Na_2SO_4). For the WD/SA co-gasification test, the ash is mainly composed of quartz, aluminosilicates (e.g. $(Ca,Na)(Al,Si)_4O_8$, $Ca_2Al_2SiO_7$) and minor content of $Ca(OH)_2$, MgO and $Ca_5(PO_4)_3OH$. This validates the previous assumption that the microalga was contaminated by sand and fine gravel particles.

3.4. Analysis of the ash transformations in wood and algae co-gasification process

Several molar ratios of the fuel ashes, in combination with the crystalline phase and the SEM/EDX analysis of the residual ashes, are used to discuss the ash transformation during the gasification process. The results are present in Table 4.

During the gasification process, the behavior of alkali metal and alkaline earth metals differs if there is a surplus of the basic components (e.g., K and Ca) in relation to the acidic components (Si and P) in the ash. Generally, alkaline earth metals will largely remain in the residual ash, whereas alkali metals will be mainly volatilized to the gas phase and form fine particulates in the colder section and cause problems like fouling and corrosion [46,51]. Previous research showed that the surplus of basic components occurs if the ratio of (K + Na + Ca + Mg)/(Si + P) is approximately larger than 3 [51]. After the reaction, the residual ash can be then categorized as ash dominated by phosphates, ash dominated by silicates, and ash dominated by both silicates and

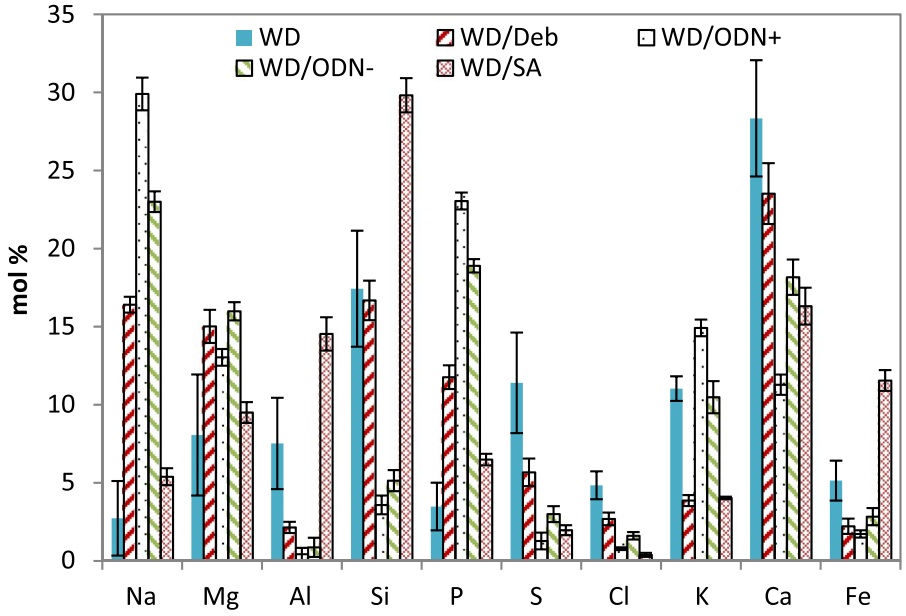

Fig. 6. Averaged elemental compositions of bottom ash samples generated from softwood and WD/algae tests, analysed by SEM/EDX on a Carbon, and Oxygen free basis.

phosphates, in the light of the relative amount of major ash-forming elements Si and P in the ash [51].

Wood has a (K + Na + Ca + Mg)/(Si + P) molar ratio of 7.1 which suggests there is a surplus basic components. The (K + Na)/(Ca + Mg) ratio (0.4) further implies the basic components are mainly composed of alkali earth metal, which will probably remain in the residual larger size fraction ash in the form of oxides, hydroxide and carbonates. This is consistent with the existence of $CaCO_3$ and MgO in the XRD results.

For the case of co-gasifying wood with algae, the algae ash accounts for > 85% of the fuel ash as a result of the extremely low ash content of the used wood biomass (0.3%). For the blends of WD/ODN + and WD/ODN-, the (K + Na + Ca + Mg)/(Si + P) molar ratio indicates the surplus of basic components. Meanwhile, the molar ratios of (K + Na)/(Ca + Mg) (2.6–3) suggest the dominated roles of alkali metal in the basic components. It is well known that [43,52] the presence of Cl facilitates the K/Na release to the gas phase as KCl/NaCl. The molar ratios of (K + Na)/Cl are in the range of 8–9 and this implies that alkali metals are released to the gas phase mainly in the form of K/Na(g), hydroxides and carbonates in a lack of Cl [29,53]. Furthermore, the blends of WD/ODN + and WD/ODN- have a low Si/P ratio (< 0.4) which suggests the residual ashes are dominated by phosphates. This was supported by the XRD results which indicate the $CaKPO_4$ was the major crystalline phase in the ashes. Under ideal conditions alkali metals will first react with P to form alkali phosphates[43]with the subsequent formation of Ca/Mg-K phosphates in the presence of alkaline earth metals [39]. Therefore the effect of phosphorus on the ash melting temperature is also closely related to the contents of Ca and Mg in the fuel. It has been proposed that a relatively high P/(Ca + Mg) molar ratio in combination with a high content of K favors the formation of low melting temperature potassium-rich phosphates [54]. For WD/ODN +, considering its high P/(Ca + Mg) molar ratio (0.9) and the high alkali metal contents, it is suggested that the available amounts of Ca and Mg are limited for the formation of refractory Ca/Mg − K phosphates. Hence, low melting temperature K/Na-rich phosphates are expected to form in the residual ash and this is supported by the existence of Na_3PO_4. Ash particles from these two tests are presented in Fig. 7. It can be observed the particles generally partially smooth and a highly porous structure which indicates a certain degree of melting during the gasification process. EDX analysis indicates that the ashes

Table 5
Crystalline phase of the residual ashes of WD/algae gasification tests, identified using XRD[a].

	Dominate phase	Major phase	Minor phase	Trace phase
WD		$CaCO_3$, $Ca_5(PO_4)_3OH$	KCl	MgO
WD/Deb		$Ca(OH)_2$	MgO, NaCl,ZSM-12/11, $CaCO_3$,$CaKPO_4$	$K_3Na(SO4)_2$, SiO_2
WD/ODN +		$CaKPO_4$, MgO	Na_3PO_4, C,SiO_2	Na_2SO_4
WD/ODN-		$CaKPO_4$, C	MgO, $Ca(OH)_2$,SiO_2	$CaCO_3$, Fe_3O_4
WD/SA		(Ca,Na) $(Al,Si)_4O_8$, SiO_2	$Ca(OH)_2$, $Ca_2Al_2SiO_7$, MgO, $Ca_5(PO_4)_3OH$	$KAlSi_3O_8$

[a] Abundance is related to the following concentration levels: dominant, > 60 wt%; major, 20–60 wt%; minor, 5–20 wt%; and trace, < 5 wt%. If more than one phase is present in aclass, they are listed in decreasing abundance.

Table 4
Ash characteristic parameters of the employed fuels and blends.

	WD	Deb	ODN +	ODN-	SA	W/Deb	W/ODN +	W/ODN-	W/SA
Ratio of algae ash to fuel ash	0	100	100	100	100	90.8	87.1	86.8	96.9
Si/P	2.5	1.4	0.1	0.3	6.3	1.4	0.2	0.4	6.3
Cl/(K + Na)	0.00	0.54	0.11	0.12	0.31	0.52	0.11	0.12	0.28
P/(Ca + Mg)	0.1	0.3	1.2	0.7	0.2	0.2	0.9	0.5	0.2
(K + Na)/Si	2.9	3.2	25.2	20.3	0.2	3.1	19.3	16.5	0.2
(Na + K)/(Ca + Mg)	0.4	1.1	3.4	4.0	0.2	1.0	2.6	3.0	0.3
(K + Na + Ca + Mg)/(Si + P)	7.1	3.5	3.4	5.9	0.7	3.6	3.6	6.0	0.8

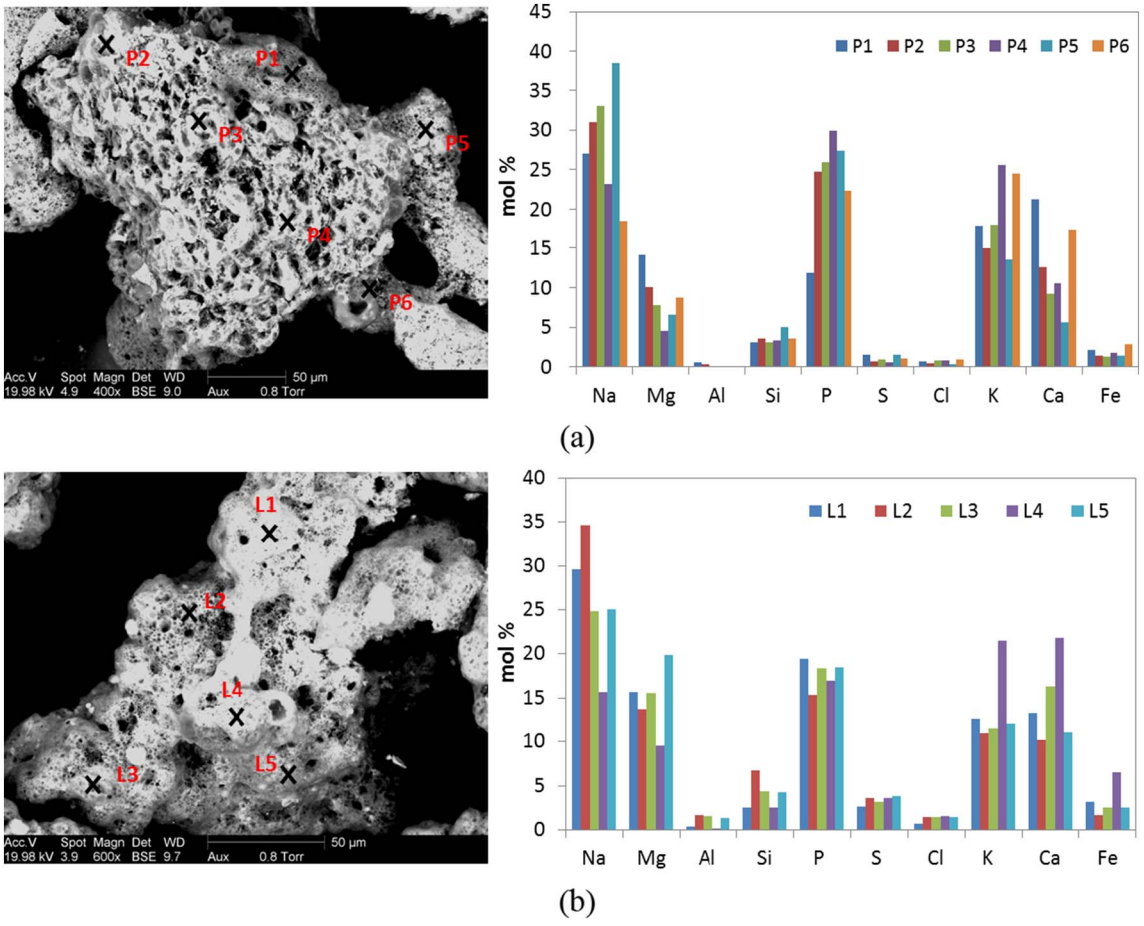

Fig. 7. Illustration and spot elemental analysis of typical residual ash particles from: (a) WD/OND+; and (b) WD/ODN-, analysed by SEM/EDX on a Carbon and Oxygen free basis.

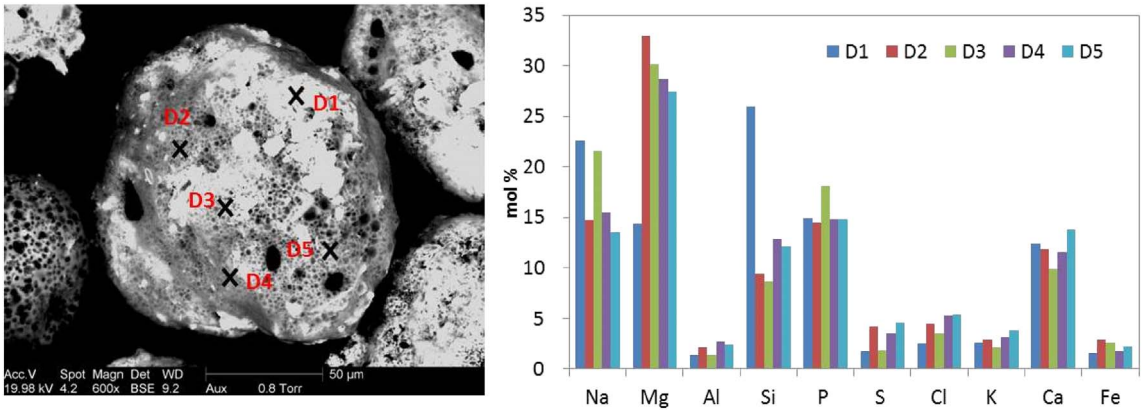

Fig. 8. Illustration and spot elemental analysis of typical residual ash particles from WD/Deb, analysed by SEM/EDX on a Carbon and Oxygen free basis.

are mainly composed of K/Na-Ca phosphates with a small content of Mg.

Similar to WD/ODN+ and WD/ODN-, the molar ratios of (K + Na + Ca + Mg)/(Si + P) and (K + Na)/(Ca + Mg) of WD/Deb suggest that the surplus of basic components consisted mainly of alkali metals. However, unlike these two tests, the Cl content is quite high for WD/Deb blends. In combination of the high Cl/(K + Na) molar ratio it can be expected that K will mainly be released to the gas phase in KCl or NaCl form. The assumption is also supported by the existence of NaCl in the residual ash from WD/Deb test. The NaCl on the ash particles is presumably derived from condensation upon cooling of the gas. The molar ratio of Si/P of the WD/Deb blend is 1.4 implying that the residual ash can be composed of both silicates and phosphates. Considering that certain amount of alkali metal would release to the gas phase, the (K + Na)/(Ca + Mg) ratio of the residual ash should be low than that of fuel ash (1.0, see Table 4). Therefore, the residual ash can be composed of alkali earth metal oxides, hydroxides, carbonates as well as Ca/Mg-K/Na silicates and phosphates. The existence of Ca $(OH)_2$, MgO, and $CaCO_3$ partially supports this assumption. However, no silicate compound and only $CaKPO_4$ was found in the XRD phases. It is inferred that part of phosphates and silicates form low melting temperature eutectics which can not be detected by XRD. The SEM/EDX results support our assumption. A representative ash particle is presented in Fig. 8. These particles generally form round shape with smooth surface which indicates melting. Spot analysis suggests that the ash particles are composed by both silicates and phosphates.

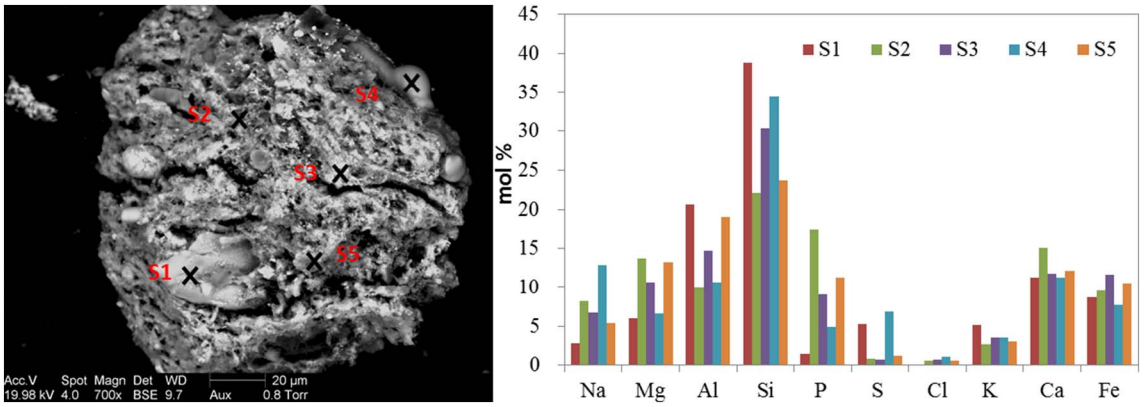

Fig. 9. Illustration and spot elemental analysis of typical residual ash particles from WD/SA, analysed by SEM/EDX on a Carbon and Oxygen free basis.

Contrary to the wood/macroalgae blends, the molar ratios of (K + Na + Ca + Mg)/(Si + P) of WD/SA blend (0.77) indicates a surplus of acidic components. Considering the very low (K + Na)/Si ratio (0.2) and Cl/(K + Na) molar ratio (0.28), most of K and Na should be fixed in the residual ash instead of releasing to gas phase under the condition of equilibrium. WD/SA has a Si/P ratio of 6.3 which indicates the residual ash could be dominated by silicates. In view of the very low (K + Na)/(Ca + Mg) molar ratio (0.25) in combination with the high Al content in the fuel ash, the residual ash is expected to be dominated by refractory Ca/Mg silicates and aluminosilicate. This is confirmed by the XRD result which shows the existence of $(Ca,Na)(Al,Si)_4O_8$, $Ca_2Al_2SiO_7$, and $KAlSi_3O_8$ in the residual ash. A representative ash particle is presented in Fig. 9. Ash particles generally have a heterogeneous and rough appearance, and EDX analysis indicates it is mainly composed of Si, Al, Ca and is likely to exist in the form of $(Ca,Na)(Al,Si)_4O_8$.

In summary, fouling and corrosion might have occurred during the entrained flow co-gasification of macroalge-wood mixture based on the analysis of the fuel ash and the collected residual ash. Microalga *Scenedesmus* contains high Si, Ca, Fe and Al contents due to the impurities infiltrating during the harvesting process, e.g. sand and fine gravel particles. These compounds could capture alkali species and potentially mitigate the fouling and corrosion problems during the gasification process. However, further fouling tests should be taken to further evaluate the fouling and corrosion tendency.

4. Conclusions

In this paper, several measurements were taken to identify the differences in composition between the algae and other solid fuels. Clear differences in the proximate and ultimate compositions were found between the cultivated algae used in this study, in particular the microalga, and macroalgae (seaweed) harvested from the marine environments. All the algae, both micro- and macro-, generally had a higher Na and P content than lignocellulosic biomass, and the microalga had a relatively high mineral content that was found to be linked to the growing environment and the impurities involved in the harvesting process.

The addition of macroalgae during gasification of softwood had limited influence on the main gas yields and carbon conversion when co-gasified with softwood. In contrast, the addition of *Scenedesmus* to softwood substantially decreased the main gas yields and carbon conversion. Moreover, presence of algae changed the residual ash composition of the wood-algae mixture, as expected.

The analysis of ash transformations of the algae during the co-gasification process provided a preliminary understanding of the behavior of the tested algae blends. Based on the analysis of the fuel ash and the collected residual ash, fouling and corrosion are presumably occurred during the co-gasification of wood/macroalgae blends. Microalga *Scenedesmus* had a high mineral content, derived from the impurities infiltrating during the harvesting process, which can potentially capture the alkali metal in the ash and mitigate fouling when gasified with softwood. The growing environment and harvesting method significantly affect the ash behavior and needs to be carefully considered in the gasification process. To further assess this, the fouling and corrosion should be taken into account in future research.

Acknowledgments

This research was supported by the Gasification of Algae: Swedish – Australian Research Platform (GASAR) Project funded through the Swedish Foundation for International Cooperation in Research and Higher Education (STINT), Natural Science Foundation of China (51706210), Provincial Key Research Project of Higher Education Institutions in Henan (Project 15600097), Doctoral Research Foundation of Zhengzhou University of Light Industry (13100368), the Swedish Strategic Research Program Bio4Energy, Australian Research Council's Linkage Projects Funding Scheme (Project LP100200616) with our industry partner SQC Pty Ltd., the Australian Government through the Australian Renewable Energy Agency (ARENA), and the Advanced Manufacturing Cooperative Research Centre (AMCRC), funded through Australian Government's Cooperative Research Centre Scheme. The financial support of J. Gust. Richert stiftelse is also appreciated. Francesco G. Gentili greatly appreciates the financial support of the Swedish Energy Agency and SP Processum. The authors also acknowledge the support of Muradel Pty Ltd. and MBD Energy. Dr. Britt Andersson at Umeå University is acknowledged for help during SEM/EDX analyses. Dr. Marie Magnusson at James Cook University is acknowledged for the culture and supply of algal pellets.

References

[1] P. McKendry, Energy production from biomass (part 1): overview of biomass, Bioresour. Technol. 83 (2002) 37–46.
[2] M.F. Demirbas, Biofuels from algae for sustainable development, Appl. Energy 88 (2011) 3473–3480.
[3] S.K. Prajapati, A. Malik, V.K. Vijay, Comparative evaluation of biomass production and bioenergy generation potential of *Chlorella* spp. through anaerobic digestion, Appl. Energy 114 (2014) 790–797.
[4] M. Ras, L. Lardon, S. Bruno, N. Bernet, J.-P. Steyer, Experimental study on a coupled process of production and anaerobic digestion of *Chlorella vulgaris*, Bioresour. Technol. 102 (2011) 200–206.
[5] R.P. John, G.S. Anisha, K.M. Nampoothiri, A. Pandey, Micro and macroalgal biomass: a renewable source for bioethanol, Bioresour. Technol. 102 (2011) 186–193.
[6] P. Biller, A.B. Ross, Potential yields and properties of oil from the hydrothermal liquefaction of microalgae with different biochemical content, Bioresour. Technol. 102 (2011) 215–225.
[7] H.K. Reddy, T. Muppaneni, S. Ponnusamy, N. Sudasinghe, A. Pegallapati, T. Selvaratnam, M. Seger, B. Dungan, N. Nirmalakhandan, T. Schaub, F.O. Holguin, P. Lammers, W. Voorhies, S. Deng, Temperature effect on hydrothermal liquefaction of *Nannochloropsis gaditana* and *Chlorella* sp. Appl. Energy 165 (2016) 943–951.
[8] J.A. Onwudili, A.R. Lea-Langton, A.B. Ross, P.T. Williams, Catalytic hydrothermal

gasification of algae for hydrogen production: composition of reaction products and potential for nutrient recycling, Bioresour. Technol. 127 (2013) 72–80.
[9] M. Aziz, T. Oda, T. Kashiwagi, Advanced energy harvesting from macro-algae—innovative integration of drying, gasification and combined cycle, Energies 7 (2014) 8217–8235.
[10] M. Aziz, T. Oda, T. Kashiwagi, Enhanced high energy efficient steam drying of algae, Appl. Energy 109 (2013) 163–170.
[11] P. McKendry, Energy production from biomass (part 3): gasification technologies, Bioresour. Technol. 83 (2002) 55–63.
[12] L. Wang, Ø. Skreiberg, M. Becidan, H. Li, Investigation of rye straw ash sintering characteristics and the effect of additives, Appl. Energy 162 (2016) 1195–1204.
[13] S. Konsomboon, S. Pipatmanomai, T. Madhiyanon, S. Tia, Effect of kaolin addition on ash characteristics of palm empty fruit bunch (EFB) upon combustion, Appl. Energy 88 (2011) 298–305.
[14] Q. Chen, J. Zhou, Q. Mei, Z. Luo, The release behavior of potassium and sodium in the biomass high-temperature entrained-flow gasification, Appl. Mech. Mater. 71-78 (2011) 2434–2441.
[15] S. Leiser, M.K. Cieplik, R. Smit, Slagging behavior of straw and corn stover and the fate of potassium under entrained-flow gasification conditions, Energy Fuel 27 (2013) 318–326.
[16] F.J. Frandsen, S.C. van Lith, R. Korbee, P. Yrjas, R. Backman, I. Obernberger, T. Brunner, M. Jöller, Quantification of the release of inorganic elements from biofuels, Fuel Process. Technol. 88 (2007) 1118–1128.
[17] M.S. Bashir, P.A. Jensen, F. Frandsen, S. Wedel, K. Dam-Johansen, J. Wadenbäck, S.T. Pedersen, Ash transformation and deposit build-up during biomass suspension and grate firing: full-scale experimental studies, Fuel Process. Technol. 97 (2012) 93–106.
[18] S.B. Hansen, P.A. Jensen, F.J. Frandsen, H. Wu, M.S. Bashir, J. Wadenbäck, B. Sander, P. Glarborg, Deposit probe measurements in large biomass-fired grate boilers and pulverized-fuel boilers, Energy Fuel 28 (2014) 3539–3555.
[19] Y. Zhu, P. Piotrowska, P.J. van Eyk, D. Boström, C.W. Kwong, D. Wang, A.J. Cole, R. de Nys, F.G. Gentili, P.J. Ashman, Cogasification of Australian Brown coal with algae in a fluidized bed reactor, Energy Fuel 29 (2015) 1686–1700.
[20] D.J. Lane, M. Zevenhoven, P.J. Ashman, P.J.v. Eyk, M. Hupa, R.d. Nys, D.M. Lewis, Algal biomass: occurrence of the main inorganic elements and simulation of ash interactions with bed material, Energy Fuel 28 (2014) 4622 – 4632.
[21] D.J. Lane, P.J.v. Eyk, P.J. Ashman, C.W. Kwong, R.d. Nys, D.A. Roberts, A.J. Cole, D.M. Lewis, Release of Cl, S, P, K, and Na during thermal conversion of algal biomass, Energy Fuel 29 (2015) 2542–2554.
[22] I.K. Alghurabie, B.O. Hasanb, B. Jackson, A. Kosminski, P.J. Ashman, Fluidized bed gasification of Kingston coal and marine microalgae in a spouted bed reactor, Chem. Eng. Res. Des. 1233 (2013) 1–11.
[23] Y. Zhu, P. Piotrowska, P.J. van Eyk, D. Boström, X. Wu, C. Boman, M. Broström, J. Zhang, C.W. Kwong, D. Wang, A.J. Cole, R. de Nys, F.G. Gentili, P.J. Ashman, Fluidized bed co-gasification of algae and wood pellets: gas yields and bed agglomeration analysis, Energy Fuel 30 (2016) 1800–1809.
[24] X. Peng, X. Ma, Z. Xu, Thermogravimetric analysis of co-combustion between microalgae and textile dyeing sludge, Bioresour. Technol. 180 (2015) 288–295.
[25] K.-C. Yang, K.-T. Wu, M.-H. Hsieh, H.-T. Hsu, C.-S. Chen, H.-W. Chen, Co-gasification of woody biomass and microalgae in a fluidized bed, J. Taiwan Inst. Chem. Eng. 44 (2013) 1027–1033.
[26] Y. Zhu, P.J. Ashman, C.W. Kwong, D. Wang, R.d. Nys, Pyrolysis characteristics and char reactivity of *Oedogonium* sp. and Loy Yang coal, Energy Fuel 29 (2015) 5047–5055.
[27] N.M.N. Qadi, A. Hidayat, F. Takahashi, K. Yoshikawa, Co-gasification kinetics of coal char and algae char under CO_2 atmosphere, Biofuels 8 (2017) 281–289.
[28] S.C.v. Lith, V. Alonso-Ramirez, P.A. Jensen, F.J. Frandsen, P. Glarborg, Release to the gas phase of inorganic elements during wood combustion. Part 1: development and evaluation of quantification methods, Energy Fuel 20 (2006) 964–978.
[29] S.C.v. Lith, P.A. Jensen, F.J. Frandsen, P. Glarborg, Release to the gas phase of inorganic elements during wood combustion. Part 2: influence of fuel composition, Energy Fuel 22 (2008).
[30] C. Higman, M. van der Burgt, Chapter 5 - gasification processes, Gasification, Second Edition, Gulf Professional Publishing, Burlington, 2008, pp. 91–191.
[31] R.J. Lawton, A.J. Cole, D.A. Roberts, N.A. Paul, R. de Nys, The industrial ecology of freshwater macroalgae for biomass applications, Algal Res. 24 (2017) 486–491.
[32] L. Mata, M. Magnusson, N.A. Paul, R. de Nys, The intensive land-based production of the green seaweeds *Derbesia tenuissima* and *Ulva ohnoi*: biomass and bioproducts, J. Appl. Phycol. 28 (2016) 365–375.
[33] N. Neveux, A.K.L. Yuen, C. Jazrawi, M. Magnusson, B.S. Haynes, A.F. Masters, A. Montoya, N.A. Paul, T. Maschmeyer, R. de Nys, Biocrude yield and productivity from the hydrothermal liquefaction of marine and freshwater green macroalgae, Bioresour. Technol. 155 (2014) 334–341.
[34] A. Cole, Y. Dinburg, B.S. Haynes, Y. He, M. Herskowitz, C. Jazrawi, M. Landau, X. Liang, M. Magnusson, T. Maschmeyer, A.F. Masters, N. Meiri, N. Neveux, R. de Nys, N. Paul, M. Rabaev, R. Vidruk-Nehemya, A.K.L. Yuen, From macroalgae to liquid fuel via waste-water remediation, hydrothermal upgrading, carbon dioxide hydrogenation and hydrotreating, Energy Environ. Sci. 9 (2016) 1828–1840.
[35] D.J. Lane, P.J. Ashman, M. Zevenhoven, M. Hupa, P.J. van Eyk, R. de Nys, O. KarlstrÖm, D.M. Lewis, Combustion behavior of algal biomass: carbon release, nitrogen release, and char reactivity, Energy Fuel 28 (2014) 41–51.
[36] R.J. Lawton, R. de Nys, N.A. Paul, Selecting reliable and robust freshwater macroalgae for biomass applications, PLoS One 8 (5) (2013) 1–7.
[37] K. Umeki, K. Kirtania, L. Chen, S. Bhattacharya, Fuel particle conversion of pulverized biomass during pyrolysis in an entrained flow reactor, Ind. Eng. Chem. Res. 51 (2012) 13973–13979.
[38] S. Wang, X.M. Jiang, X.X. Han, H. Wang, Fusion characteristic study on seaweed biomass ash, Energy Fuel 22 (2008) 2229–2235.
[39] A.B. Ross, J.M. Jones, M.L. Kubacki, T. Bridgeman, Classification of macroalgae as fuel and its thermochemical behaviour, Bioresour. Technol. 99 (2008) 6494–6504.
[40] S.V. Vassilev, D. Baxter, L.K. Andersen, C.G. Vassileva, An overview of the chemical composition of biomass, Fuel 89 (2010) 913–933.
[41] P.J. Van Eyk, A. Kosminski, P.J. Ashman, Control of agglomeration and defluidization during fluidized-bed combustion of south Australian low-rank coals, Energy Fuel 26 (2012) 118–129.
[42] A.R. McLennan, G.W. Bryant, B.R. Stanmore, T.F. Wall, Ash formation mechanisms during pf combustion in reducing conditions, Energy Fuel 14 (2000) 150–159.
[43] D. Bostrom, N. Skoglund, A. Grimm, C. Boman, M. Ohman, M. Brostrom, R. Backman, Ash transformation chemistry during combustion of biomass, Energy Fuel 26 (2012) 85–93.
[44] H. Li, K. Han, Q. Wang, C. Lu, Influence of ammonium phosphates on gaseous potassium release and ash-forming characteristics during combustion of biomass, Energy Fuel 29 (2015) 2555–2563.
[45] A. Grimm, N. Skoglund, D. BostrÖm, C. Boman, M. Öhman, Influence of phosphorus on alkali distribution during combustion of logging residues and wheat straw in a bench-scale fluidized bed, Energy Fuel 26 (2012) 3012–3023.
[46] Y. Niu, H. Tan, S.e. Hui, Ash-related issues during biomass combustion: alkali-induced slagging, silicate melt-induced slagging (ash fusion), agglomeration, corrosion, ash utilization, and related countermeasures, Prog. Energy Combust. Sci. 52 (2016) 1–61.
[47] M. Hupa, Ash-related issues in fluidized-bed combustion of biomasses: recent research highlights, Energy Fuel 26 (2012) 4–14.
[48] H. Yang, R. Yan, H. Chen, D.H. Lee, C. Zheng, Characteristics of hemicellulose, cellulose and lignin pyrolysis, Fuel 86 (2007) 1781–1788.
[49] T. Hanaoka, S. Inoue, S. Uno, T. Ogi, T. Minowa, Effect of woody biomass components on air-steam gasification, Biomass Bioenergy 28 (2005) 69–76.
[50] P.A. Jensen, F.J. Frandsen, J. Hansen, K. Dam-Johansen, N. Henriksen, S. Hörlyck, SEM investigation of Superheater deposits from biomass-fired boilers, Energy Fuel 18 (2004) 378–384.
[51] M. Díaz-Ramírez, C. Boman, F. Sebastián, J. Royo, S. Xiong, D. Boström, Ash characterization and transformation behavior of the fixed-bed combustion of novel crops: poplar, brassica, and cassava fuels, Energy Fuel 26 (2012) 3218–3229.
[52] J.M. Johansen, J.G. Jakobsen, F.J. Frandsen, P. Glarborg, Release of K, Cl, and S during pyrolysis and combustion of high-chlorine biomass, Energy Fuel 25 (2011) 4961–4971.
[53] J.N. Knudsen, P.A. Jensen, K. Dam-Johansen, Transformation and release to the gas phase of Cl, K, and S during combustion of annual biomass, Energy Fuel 18 (2004) 1385–1399.
[54] L. Wang, J.E. Hustad, M. Grønli, Sintering characteristics and mineral transformation behaviors of corn cob ashes, Energy Fuel 26 (2012) 5905–5916.